# Magnetic Tunnel Junctions Incorporating a Near-Zero-Moment Ferromagnetic Semiconductor

H. Warring,[1] H. J. Trodahl,[1] N. O. V. Plank,[1] F. Natali,[1] S. Granville,[2] and B. J. Ruck[1]

[1]*The MacDiarmid Institute for Advanced Materials and Nanotechnology, School of Chemical and Physical Sciences, Victoria University of Wellington, P.O. Box 600, Wellington 6140, New Zealand*

[2]*The MacDiarmid Institute for Advanced Materials and Nanotechnology, Robinson Research Institute, P.O. Box 33436, Petone 5046, New Zealand*

(Received 23 February 2016; revised manuscript received 30 July 2016; published 3 October 2016)

We present a fully semiconductor-based magnetic tunnel junction that uses spin-orbit coupled materials made of *intrinsic* ferromagnetic semiconductors. Unlike more common approaches, one of the electrodes consists of a near-zero magnetic-moment ferromagnetic semiconductor, samarium nitride, with the other electrode composed of the more conventional ferromagnetic semiconductor gadolinium nitride. Fabricated tunnel junctions show a magnetoresistance as high as 200%, implying strong spin polarization in both electrodes. In contrast to conventional tunnel junctions, the resistance is largest at high fields, a direct result of the orbital-dominant magnetization in samarium nitride that requires that the spin in this electrode must align opposite to that in the gadolinium nitride when the magnetization is saturated. The magnetoresistance at intermediate fields is controlled by the formation of a twisted magnetization phase in the samarium nitride, a direct result of the orbital-dominant ferromagnetism. Thus, an alternative type of functionality can be brought to magnetic tunnel junctions by the use of different electrode materials, in contrast to the usual focus on tuning the barrier properties.

DOI: 10.1103/PhysRevApplied.6.044002

## I. INTRODUCTION

Magnetic tunnel junctions consisting of a ferromagnet-insulator-ferromagnet stack have produced major technological impacts, forming the basis for both modern hard-drive read heads and the emergent technology of tunneling magnetoresistive magnetic random access memory. They have also served as an important testing ground for fundamental theories of spin transport [1]. The tunnel magnetoresistance is defined by $\mathrm{TMR} = (R_{ap} - R_p)/R_p$, with $R_{ap}$ and $R_p$ the resistance measured when the spin alignment in the conduction channels of the two ferromagnetic electrodes are antiparallel or parallel, respectively. In conventional ferromagnetic conductors that alignment is signaled by the magnetization, but as detailed below, the strong spin-orbit interaction in the samarium $4f$ shell leads to the opposite alignment in samarium nitride (SmN). If the tunneling process conserves spin, then the resistance of the junction is minimized when the electrodes have parallel spin orientation. The most widely exploited electrode materials in magnetic tunnel junctions are ferromagnetic transition metals such as iron, nickel, cobalt, and their alloys [1]. However, these conventional transition metal-based ferromagnets have only partial spin polarization, limiting the TMR. Recent gains in transition metal-based device performance have been driven by exploiting new barrier technologies using MgO, where the wave functions in the electrodes and the barrier are matched such that tunneling of the most highly polarized carriers is favored. To further enhance the TMR, fully spin-polarized half-metallic ferromagnets such as Heusler alloys, manganites, or dilute magnetic semiconductors have been employed [2–7]. TMR values of more than 6000% have been observed in such manganite systems at low temperatures [4,5].

Alongside the progress on tunnel junctions have come new discoveries on the interaction between the electron's spin and orbital motion, including much progress in understanding the anomalous and spin Hall effects [8,9], and the recent development of spin orbitronics [10]. It has become clear that an increased control of magnetization dynamics can be obtained by incorporating orbital effects in addition to the usual spin contribution to the magnetism. Nonetheless, to date this has not extended to the use of spin-orbit coupled materials in the electrodes of magnetic tunnel junctions. Of particular interest are systems where the spin and orbital moments cancel, resulting in zero net moment. Such materials offer promise in devices as they are free from stray fields and relatively immune to demagnetizing forces, making them of interest in densely packed memory elements. The critical current required to switch a magnetic random access memory element using spin-transfer torque is expected to be proportional to the saturation magnetization of the free layer, which has further enhanced interest in zero-moment ferromagnets [11,12].

In the past decade, evidence has accumulated that the rare-earth nitride series includes several ferromagnetic semiconductors [13–19], which makes them of interest as spin-polarized injectors and active elements in spintronic applications. Incorporation of gadolinium nitride (GdN) as

 

nanoislands in gallium nitride (GaN) has already been demonstrated [20], work that suggests potential future advances in spin-polarized optoelectronics. There are also reports of tunneling structures incorporating highly spin polarizing GdN and dysprosium nitride (DyN) as spin filter layers [21,22]. Furthermore, unlike the $3d$ and $4d$ magnetism in transition metal ions, the rare earths do not feature full orbital quenching so that the net moment includes both spin and orbital contributions. The total moment is then larger, smaller, or even oriented antiparallel to the spin moment [23–25].

The potential of the rare-earth nitrides is enhanced by their common (NaCl) crystal structure and similar lattice constants, which permit epitaxial compatibility among them, and by their epitaxial compatibility with lanthanum nitride (LaN), GaN, and aluminium nitride (AlN), three obvious compositions for tunneling barriers [16,26].

Here, we report novel tunneling characteristics in magnetic tunnel junctions with electrodes made from two contrasting members of the series, GdN and SmN. GdN has occupied the role as prototypical rare-earth nitride, with much more work done on it than has been afforded any of the rest of the series. Gd lies at the center of the lanthanide series, and the trivalent Gd ion in GdN has an exactly half-filled $4f$ shell, with zero orbital angular momentum ($L = 0$), fully aligned spins ($S = 7/2$), and a magnetic moment of 7 $\mu_B$ residing purely in the spin component [27]. It thus resembles the spin-only magnetism that is also characteristic of transition-metal compounds. However, the spherically symmetric ($L = 0$) orbital function results in a small crystal anisotropy, with coercive fields as low as $10^{-3}$ T having been reported [13]. In contrast, $Sm^{3+}$ features $(L, S)$ of $(5, 5/2)$, and in the presence of a strong spin-orbit interaction the Hund's rule ground state has opposing spin and orbital alignment. This leads to a small magnetic moment of only 0.8 $\mu_B$ in the free ion [27]. That moment is further reduced by the crystal field and exchange interaction in SmN to yield a ferromagnetic moment of only 0.035 $\mu_B$ per formula unit [23,24]; to our knowledge, this is the smallest ferromagnetic magnetization in any stoichiometric compound. The small moment results from an almost complete cancellation of spin and orbital contributions [24]. Significantly it is the orbital moment which dominates weakly in SmN. Its net magnetization is then directed in opposition to the $4f$ spin magnetic moment, which will be seen below to have important consequences in GdN/AlN/SmN devices. The coercive field of SmN is larger than 6 T at low temperatures [23], resulting from a stronger crystal anisotropy and much weaker Zeeman interaction than in GdN, again with important consequences. The strong spin polarization of the $4f$ shell in both GdN and SmN results in a large exchange splitting of the conduction band, such that doped charge carriers are expected to be highly spin polarized [13,28].

## II. EXPERIMENTAL DETAILS

GdN/GaN/GdN, GdN/AlN/GdN, and GdN/AlN/SmN tunneling structures are formed by photolithography in a cross-contact geometry, as shown schematically in Fig. 1(a). Note that the use of both GaN and AlN in the insulating barriers permits tuning of the barrier height, and that otherwise one expects, and we find, that the two barrier choices are interchangeable. A narrow (100-$\mu$m) gold contact strip is deposited onto a sapphire substrate and patterned using photolithography and a metal lift-off process. A second photolithography step is performed and Gd is deposited at 0.02–0.05 nm/s by vapor deposition under a nitrogen pressure of $1–10 \times 10^{-4}$ mbar, resulting in the formation of GdN. Ga or Al are deposited in the presence of activated nitrogen from a Kaufmann cell to grow the insulating GaN or AlN barriers followed by a second GdN or SmN layer, with SmN grown in the same manner as GdN. The structures are capped by Gd metal both to protect the structure from oxidation and to provide electrical contact to the top of the structure. After the growth of the tunnel junction and the Gd layer the photoresist is removed via a second lift-off process.

The typical SEM image of Fig. 1(b) shows that the insulating layer is no thicker than 5 nm, while all other layers are close to 100 nm thick. X-ray reflectometry performed on a GaN layer grown under similar conditions yields a thickness of ~5 nm, consistent with the SEM results. The device is deposited at ambient temperature, which results in GdN layers that are smooth and strongly (111) textured [14]. Ambient-temperature deposited SmN is much less strongly textured, and, unsurprisingly, we could not prepare smooth structures showing clear

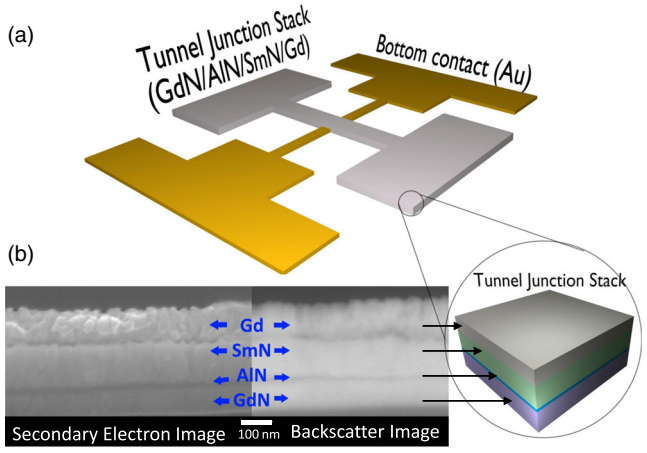


FIG. 1. (a) Schematic illustration of the entire magnetic-tunnel-junction geometry, where the "tunnel-junction stack" is shown at lower right. The tunnel-junction area is 100 $\mu$m × 200 $\mu$m. (b) Cross-section SEM images of a GdN/AlN/SmN tunnel junction obtained by both backscatter and secondary electron imaging. The backscatter image highlights the AlN layer.

tunneling characteristics with SmN as the substrate for the AlN insulating barrier.

## III. RESULTS AND DISCUSSION

The current-voltage ($I$-$V$) characteristics of a GdN/AlN/SmN tunnel junction shown in Fig. 2 are well described by the Simmons square barrier model [29,30], from which we extract a barrier width of 2 nm. This is consistent with the average AlN layer thickness of ~5 nm, where the tunneling is dominated by the thinnest parts of the barrier. The fitted barrier height is about 1.6 eV (see Fig. 2 inset). The Fermi level in GdN is close to the conduction-band minimum [14], implying that the rare-earth nitride conduction band sits slightly above the middle of the 6.2-eV AlN gap. This band offset is consistent with recent calculations of Kagawa *et al.* [31], who find the GdN Fermi level lies close to midgap for GaN. Future investigation employing more sophisticated tunneling models may provide further insight into the actual barrier-height amplitude, as well as the density of states in the electrodes [32].

The strikingly unusual properties of the GdN/AlN/SmN tunnel junction are illustrated by the low-temperature magnetoresistance data shown in Fig. 3(a). The magnetoresistance is as large as 140% with the field in plane and nearly 200% with the field out of plane. It is important to note that the device resistance is largest at fields high enough to saturate the magnetization of both layers, which is *opposite* to the behavior of conventional tunnel junctions. As illustrated in Fig. 4 the positive magnetoresistance is a direct result of the orbital-dominant nature of the magnetism in SmN: at high fields it is the net, orbital-dominant magnetic moment that aligns with the field, which then forces the spin magnetic moment to align opposite to the field. On the other hand, the purely spin-based moment in GdN is aligned with the field, and thus high fields lead to opposite spin alignment across the tunnel barrier and in turn a high resistance. This novel behavior is a clear demonstration that the device is operating in the tunneling regime, with the very large magnetoresistance indicating strong spin polarization in the rare-earth nitride electrodes. The magnetoresistance observed in GdN/I/GdN ($I$ = GaN, AlN) control junctions, illustrated in Fig. 5 for a junction with area 100 $\mu$m × 200 $\mu$m and layer thicknesses of 60 nm for the GdN layers, is negative, smaller, and shows no signs of the interesting features observed in the SmN system. The barrier thickness is nominally the same as for the GdN/AlN/SmN junction, but the resistance of the GdN/GaN/GdN junction is larger, presumably because the actual barrier thickness is in fact slightly larger.

More unusual features are revealed in the magnetoresistance at lower fields. A pronounced dip occurs between 1 and 4 T, with no evidence for hysteresis between upward and downward field sweeps. The lack of dependence on the field orientation of this feature implies it originates in changes in the magnetization of the SmN electrode whose

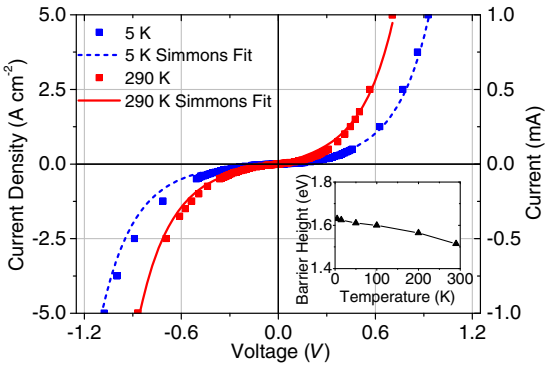


FIG. 2. Current-voltage characteristics for a GdN/AlN/SmN tunnel junction fitted using the Simmons tunneling model. Inset: Modeled barrier height (average of forward and reverse current) plotted against temperature.

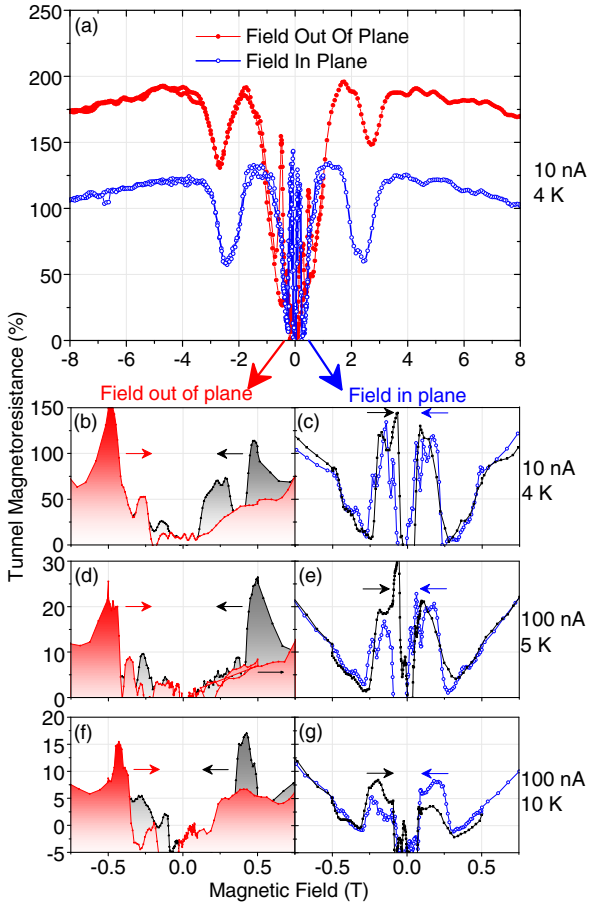


FIG. 3. (a) Magnetoresistance data from a GdN/AlN/SmN tunnel junction obtained from −8 T to 8 T at 4 K in both the in-plane and out-of-plane orientations with a measurement current of 10 nA. (b)–(g) Tunnel magnetoresistance data at low fields measured both in increasing and decreasing fields using different currents and temperatures.

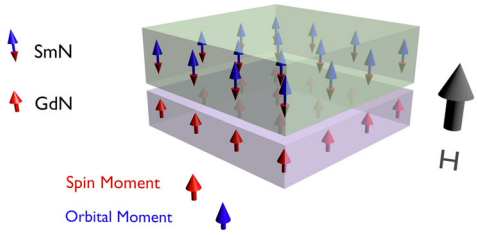


FIG. 4. Schematic diagram of the spin and orbital parts of the magnetic moments when the tunnel junction is in the high resistance state in a large applied field. For SmN the magnetic moment is dominated by the orbital contribution, so the spin moment aligns opposite to the field.

near-vanishing moment leads to a very small shape anisotropy. Its appearance below 4 T is consistent with the magnitude of the coercive field expected for SmN [23,24].

The region closer to zero field is expanded in Figs. 3(b)–3(g), where large and reproducible changes are seen in the magnetoresistance that now depend on the field orientation. With the field in the film plane the magnetoresistance shows strong maxima of over 140% either side of zero field. These are reminiscent of those that occur in conventional magnetic tunnel junctions when the spin orientation of the electrodes are in opposition [1], but crucially here the maxima occur on both the positive and negative side of zero field, independent of the direction of field sweep. The field-out-of-plane data show similar strong features, but at somewhat larger fields, and in this case the maxima are hysteretic. Most surprisingly, the hysteresis is in the opposite sense to that conventionally expected, i.e., the maxima occur on decreasing rather than increasing field strength, implying that one of the electrodes switches spin orientation before, rather than after, the field passes through zero. All of the low-field features are still present when the current is increased by an order of magnitude, although their magnitude is reduced substantially [Figs. 3(d)–3(g)]. Such a decrease of the TMR value with increasing bias voltage is common in most, though not all, tunnel junctions [33]. The reproducibility of the peak structures at different fields and temperatures makes it clear that they are not simply the result of instrumental noise. This conclusion is further supported by the fact that the high-field data show little noise.

In Fig. 6 we examine the temperature-dependent resistance of the GdN/AlN/SmN tunnel junction. Under low current a clear feature is observed near the ≈50 K Curie temperature of the GdN electrodes, with an additional feature seen near the ≈30 K Curie temperature of SmN. These features are caused by exchange splitting of the energy bands as the rare-earth nitrides enter the ferromagnetic state [13,14]. The resistance is several orders of magnitude larger than would be expected for SmN or GdN in the absence of a tunnel barrier [13], so clearly transport through the tunnel junction is dominated by the presence of the barrier layer. However, the presence of the exchange-splitting features emphasizes again that the density of states in the electrodes also has an important influence on the device characteristics. For larger applied currents, and hence voltages, the features are less noticeable because states further from the Fermi level are probed. The separate resistance features associated with GdN and SmN show that these layers maintain their individual magnetic character.

The GdN/AlN/SmN magnetoresistance data are in marked contrast to the conventional behavior of magnetic tunnel junctions, which are opposite in sign and do not show the same detailed structure as a function of field. Overall, the data imply a complicated switching of the spin orientations within the SmN and GdN electrodes, so a direct investigation of the magnetization is clearly of interest. The vanishingly small SmN magnetic moment is entirely masked by the large GdN moment, so conventional magnetization measurements are not useful. However, we have used x-ray magnetic circular dichroism to probe the Gd and Sm moments independently both in coupled GdN/SmN bilayers and in GdN/I/SmN

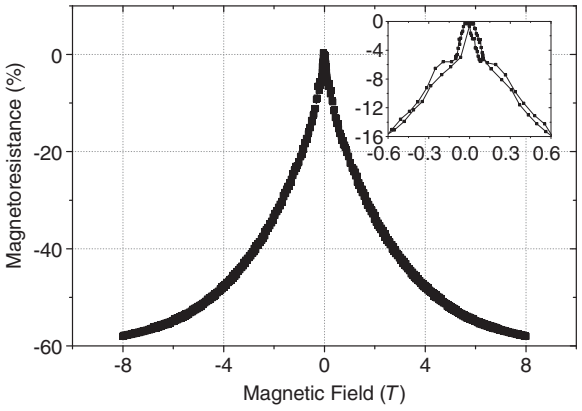


FIG. 5. Magnetoresistance data at 4 K from a GdN/GaN/GdN tunnel junction obtained with measurement current 50 nA and the field applied parallel to the layers. Inset: Low-field data.

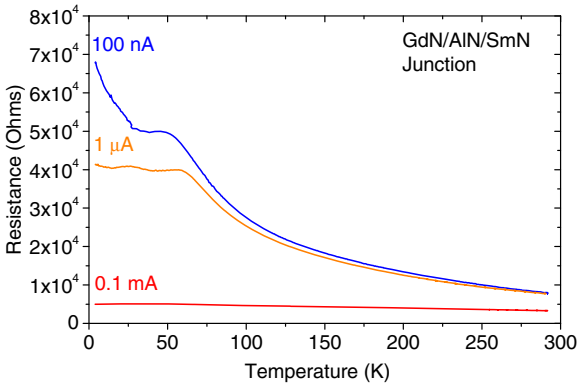


FIG. 6. Temperature-dependent resistance of a GdN/AlN/SmN tunnel junction, measured using various applied currents.

heterostructures analogous to the present tunneling structures [24,34]. The results reveal that SmN layers form a twisted magnetization phase when the spins at one interface are pinned, for example, by an exchange interaction with a neighboring ferromagnet [34], while the layer is simultaneously subject to an applied magnetic field that seeks to align the spins in the opposite direction. The result is a magnetization that rotates as a function of distance from the interface, similar to an exchange spring. The small magnetic moment of SmN, and the corresponding weak Zeeman interaction, yield a length scale for the rotation of several tens of nanometers in fields of order one Tesla.

It is likely that such a twisted phase forms in the SmN layer of the magnetic tunnel junction described here, where the interface pinning comes from the top Gd electrode that is in direct contact with the SmN. A twisted phase propagating through the SmN to the tunnel barrier with a length scale that decreases with increasing applied field then leads to the intermediate field oscillations observed in the magnetoresistance. The exact origin of the magnetoresistance oscillations at low field is less certain, but the strong dependence on field orientation strongly suggest that they originate in magnetization dynamics within the GdN layer which has strong shape anisotropy, and which also has a coercive field in the low-field range [14]. This scenario is supported by the appearance of structure at similar fields in the GdN/I/GdN tunneling device, as seen in the inset of Fig. 5. Observations in similar ferromagnetic semiconductor systems attribute the spontaneous magnetization reversal to the large ratio between anisotropy and coercive fields. With the field out of plane, even a small in-plane component can result in the magnetization switching between in-plane easy directions [35].

## IV. CONCLUSIONS

In summary, the data presented here for a magnetic tunnel junction incorporating a near-zero-moment ferromagnet demonstrate the possibility of bringing an alternative functionality to these devices by exploiting different spin and orbital magnetic properties in the electrodes. We find an exceptionally large magnetoresistance for a polycrystalline tunnel junction, indicative of strong spin polarization in the electrodes. The positive sign of the magnetoresistance is a direct result of the use of the orbital-dominant ferromagnet SmN as an electrode material. This zero-moment ferromagnet also leads to an unusual field-dependent structure in the magnetoresistance data. The spintronics potential of moment-free ferromagnets has recently been highlighted also in a half-metallic Heusler system [11,12], where the moment cancellation comes from two competing spin contributions rather than competing spin and orbital moments. Investigating the similarities and differences in devices based on the two types of zero-moment systems promises to provide much insight into their physics.

## ACKNOWLEDGMENTS

We acknowledge funding from the New Zealand Foundation for Research, Science and Technology (VICX0808), the Marsden Fund (13-VUW-1309), and the MacDiarmid Institute for Advanced Materials and Nanotechnology, funded by the New Zealand Centres of Excellence Fund. The authors would also like to thank Jay Chan and Dr. Olly Pantoja for assistance in performing x-ray reflectivity measurements.

[1] H. J. M. Swagten, in *Handbook of Magnetic Materials*, edited by K. H. J. Buschow (Elsevier, Amsterdam, 2007), Vol. 17, Chap. 1, pp. 1–121.
[2] Warren E. Pickett and Jagadeesh S. Moodera, Half metallic magnets, Phys. Today **54**, No. 5, 39 (2001).
[3] J. S. Parker, S. M. Watts, P. G. Ivanov, and P. Xiong, Spin Polarization of $CrO_2$ at and across an Artificial Barrier, Phys. Rev. Lett. **88**, 196601 (2002).
[4] M. Bowen, M. Bibes, A. Barthélémy, J.-P. Contour, A. Anane, Y. Lemaître, and A. Fert, Nearly total spin polarization in $La_{2/3}Sr_{1/3}MnO_3$ from tunneling experiments, Appl. Phys. Lett. **82**, 233 (2003).
[5] M. Bowen, A. Barthélémy, M. Bibes, E. Jacquet, J.-P. Contour, A. Fert, D. Wortmann, and S. Blügel, Half-metallicity proven using fully spin-polarized tunnelling, J. Phys. Condens. Matter **17**, L407 (2005).
[6] M. Tanaka and Y. Higo, Large Tunneling Magnetoresistance in GaMnAs/AlAs/GaMnAs Ferromagnetic Semiconductor Tunnel Junctions, Phys. Rev. Lett. **87**, 026602 (2001).
[7] H. Saito, S. Yuasa, and K. Ando, Origin of the Tunnel Anisotropic Magnetoresistance in $Ga_{1-x}Mn_xAs$/ZnSe/$Ga_{1-x}Mn_xAs$ Magnetic Tunnel Junctions of II-VI/III-V Heterostructures, Phys. Rev. Lett. **95**, 086604 (2005).
[8] Naoto Nagaosa, Jairo Sinova, Shigeki Onoda, A. H. MacDonald, and N. P. Ong, Anomalous Hall effect, Rev. Mod. Phys. **82**, 1539 (2010).
[9] Jairo Sinova, Sergio O. Valenzuela, J. Wunderlich, C. H. Back, and T. Jungwirth, Spin Hall effects, Rev. Mod. Phys. **87**, 1213 (2015).
[10] A Manchon, Spin-orbitronics: A new moment for Berry, Nat. Phys. **10**, 340 (2014).
[11] H. Kurt, K. Rode, P. Stamenov, M. Venkatesan, Y.-C. Lau, E. Fonda, and J. M. D. Coey, Cubic $Mn_2Ga$ Thin Films: Crossing the Spin Gap with Ruthenium, Phys. Rev. Lett. **112**, 027201 (2014).
[12] Naganivetha Thiyagarajah, Yong-Chang Lau, Davide Betto, Kiril Borisov, J. M. D. Coey, Plamen Stamenov, and Karsten Rode, Giant spontaneous Hall effect in zero-moment $Mn_2Ru_xGa$, Appl. Phys. Lett. **106**, 122402 (2015).
[13] F. Natali, B. J. Ruck, N. O. V. Plank, H. J. Trodahl, S. Granville, C. Meyer, and W. R. L. Lambrecht, Rare-earth mononitrides, Prog. Mater. Sci. **58**, 1316 (2013).
[14] S. Granville, B. J. Ruck, F. Budde, A. Koo, D. J. Pringle, F. Kuchler, A. R. H. Preston, D. H. Housden, N. Lund, A. Bittar, G. V. M. Williams, and H. J. Trodahl, Semiconducting ground state of GdN thin films, Phys. Rev. B **73**, 235335 (2006).

[15] D. L. Binh, B. J. Ruck, F. Natali, H. Warring, H. J. Trodahl, E.-M. Anton, C. Meyer, L. Ranno, F. Wilhelm, and A. Rogalev, Europium Nitride: A Novel Diluted Magnetic Semiconductor, Phys. Rev. Lett. **111**, 167206 (2013).

[16] F. Natali, N. O. V. Plank, J. Galipaud, B. J. Ruck, H. J. Trodahl, F. Semond, S. Sorieul, and L. Hirsch, Epitaxial growth of GdN on silicon substrate using an AlN buffer layer, J. Cryst. Growth **312**, 3583 (2010).

[17] D. L. Cortie, J. D. Brown, S. Brück, T. Saerbeck, J. P. Evans, H. Fritzsche, X. L. Wang, J. E. Downes, and F. Klose, Intrinsic reduction of the ordered $4f$ magnetic moments in semiconducting rare-earth nitride thin films: DyN, ErN, and HoN, Phys. Rev. B **89**, 064424 (2014).

[18] H. Yoshitomi, S. Kitayama, T. Kita, O. Wada, M. Fujisawa, H. Ohta, and T. Sakurai, Optical and magnetic properties in epitaxial GdN thin films, Phys. Rev. B **83**, 155202 (2011).

[19] I. L. Farrell, R. J. Reeves, A. R. H. Preston, B. M. Ludbrook, J. E. Downes, B. J. Ruck, and S. M. Durbin, Tunable electrical and optical properties of hafnium nitride thin films, Appl. Phys. Lett. **96**, 071914 (2010).

[20] Sriram Krishnamoorthy, Thomas F. Kent, Jing Yang, Pil Sung Park, Roberto C. Myers, and Siddharth Rajan, GdN Nanoisland-based GaN tunnel junctions, Nano Lett. **13**, 2570 (2013).

[21] P. K. Muduli, Avradeep Pal, and Mark G. Blamire, Crossover from diffusive to tunneling regime in NbN/DyN/NbN ferromagnetic semiconductor tunnel junctions, Phys. Rev. B **89**, 094414 (2014).

[22] Kartik Senapati, Mark G. Blamire, and Zoe H. Barber, Spin-filter Josephson junctions, Nat. Mater. **10**, 849 (2011).

[23] C. Meyer, B. J. Ruck, J. Zhong, S. Granville, A. R. H. Preston, G. V. M. Williams, and H. J. Trodahl, Near-zero-moment ferromagnetism in the semiconductor SmN, Phys. Rev. B **78**, 174406 (2008).

[24] Eva-Maria Anton, B. J. Ruck, C. Meyer, F. Natali, Harry Warring, Fabrice Wilhelm, A. Rogalev, V. N. Antonov, and H. J. Trodahl, Spin/orbit moment imbalance in the near-zero moment ferromagnetic semiconductor SmN, Phys. Rev. B **87**, 134414 (2013).

[25] E.-M Anton, J. F. McNulty, B. J. Ruck, M. Suzuki, M. Mizumaki, V. N. Antonov, J. W. Quilty, N. Strickland, and H. J. Trodahl, NdN: An intrinsic ferromagnetic semiconductor, Phys. Rev. B **93**, 064431 (2016).

[26] M. A. Scarpulla, C. S. Gallinat, S. Mack, J. S. Speck, and A. C. Gossard, GdN (1 1 1) heteroepitaxy on GaN (0 0 0 1) by $N_2$ plasma and $NH_3$ molecular beam epitaxy, J. Cryst. Growth **311**, 1239 (2009).

[27] J. H. Van Vleck, *The Theory of Electric and Magnetic Susceptibilities*, The International Series of Monographs on Physics (Oxford University Press, Oxford, 1952).

[28] P Larson, Walter R. L. Lambrecht, Athanasios Chantis, and Mark van Schilfgaarde, Electronic structure of rare-earth nitrides using the LSDA+U approach: Importance of allowing $4f$ orbitals to break the cubic crystal symmetry, Phys. Rev. B **75**, 045114 (2007).

[29] John G. Simmons, Generalized formula for the electric tunnel effect between similar electrodes separated by a thin insulating film, J. Appl. Phys. **34**, 1793 (1963).

[30] John G. Simmons, Generalized Thermal $J$-$V$ Characteristic for the Electric Tunnel Effect, J. Appl. Phys. **35**, 2655 (1964).

[31] Toshiya Kagawa and Hannes Raebiger, Schottky Barrier Formation and Strain at the (011) GdN/GaN Interface from First Principles, Phys. Rev. Applied **2**, 054009 (2014).

[32] F. Schleicher *et al.*, Localized states in advanced dielectrics from the vantage of spin- and symmetry-polarized tunnelling across MgO, Nat. Commun. **5**, 1 (2014).

[33] J.-M. De Teresa, A. Barthélémy, A. Fert, J.-P. Contour, F. Montaigne, and P. Seneor, Role of metal-oxide interface in determining the spin polarization of magnetic tunnel junctions, Science **286**, 507 (1999).

[34] J. F. McNulty, E.-M. Anton, B. J. Ruck, F. Natali, H. Warring, F. Wilhelm, A. Rogalev, M. M. Soares, N. B. Brookes, and H. J. Trodahl, Twisted phase of the orbital-dominant ferromagnet SmN in a GdN/SmN heterostructure, Phys. Rev. B **91**, 174426 (2015).

[35] F. Matsukura, M. Sawicki, T. Dietl, D. Chiba, and H. Ohno, Magnetotransport properties of metallic (Ga,Mn)As films with compressive and tensile strain, Physica (Amsterdam) **21E**, 1032 (2004).